Optimizing Transition Edge Sensors for High-Resolution X-ray Spectroscopy

Tarek Saab*, Simon R. Bandler, Kevin Boyce, James A. Chervenak, Enectali Figueroa-Feliciano, Naoko Iyomoto, Richard L. Kelley, Caroline A. Kilbourne, Frederick S. Porter and John E. Sadleir

NASA Goddard Space Flight Center, Greenbelt, MD 20771, USA

Abstract. Transition Edge Sensors (TES) have found applications as astronomical detectors ranging from the microwave to the gamma ray energy bands. Each energy band, however, imposes a different set of requirements on the TES such as energy and timing resolution, focal plane coverage, and the mechanisms by which the signal is coupled to the detector. This paper focuses on the development of TESs optimized for the 0.1-10 keV energy range at the NASA Goddard Space Flight Center. Such detectors are suitable candidates for some of the upcoming X-ray observatories such as NeXT and Constellation-X. Ongoing efforts at producing, characterizing, and modeling such devices, as well as the latest results, are discussed.

Keywords: X-ray, Spectroscopy, Microcalorimeter, TES, Noise
PACS: 07.85.Nc,95.55.Ka , 74.40.+k

INTRODUCTION

High resolution X-ray spectroscopy offers a unique window on many areas of cosmology and astrophysics. Following up on the wealth of information learned from the Chandra and XMM-Newton missions [1], the Astro-E2 mission [2] is being prepared for launch in summer of 2005, featuring a high energy resolution non-dispersive x-ray spectrometer based on Si thermistor microcalorimeters. Missions in the planning stages, such as NeXT, Constellation-X, and XEUS, are already looking beyond Astro-E2 in terms of energy resolution, timing, and imaging capabilities. Table 1 compares the envisaged detector performance for these missions. Microcalorimeters based on Transition Edge Sensor (TES) technology are an excellent candidate to achieve these goals. In this paper we will present some of the results of the TES microcalorimeter development carried out at NASA Goddard Space Flight Center.

TABLE 1. Comparison of the major performance requirements of the soft x-ray spectrometer for the Astro-E2, NeXT, and Constellation-X missions. The specification for all missions apply to an energy band of $\sim$0.1 - 10 keV.

	Pixel Size [μm]	**Num Pixels**	**Energy Res. [eV]**	**Count Rate [Hz]**
Astro-E2	600	32	6	$\sim$10
NeXT	800	400	4	$\sim$100
Con-X	250	1000	4	$\sim$1000

TRANSITION EDGE SENSORS

A Transition Edge Sensor (TES) consists of a superconducting film whose large variation in resistance at the superconducting critical temperature is utilized as a sensitive thermometer. A good description of the principles of TESs and electrothermal feedback can be found in [3]. The TESs being developed at NASA GSFC use Mo/Au bilayers as the superconducting film, suspended on a silicon nitride membrane from the main Si chip. The advantages of such a scheme lie in the ability to control the T_c of the TES by adjusting the relative thicknesses of the Mo and Au film. In addition, the thermal conductance between the TES and the heat sink ($G_{TES-Bath}$) can be controlled by varying the perimeter and thickness of the silicon nitride membrane. This level of control allows the flexibility to meet the various x-ray mission specifications, since the abovementioned TES parameters, in addition to α, a measure of the steepness of the transition, can be optimized to produce the required performance.

Attached Absorbers

One of the primary requirements of the x-ray telescopes is a high detection efficiency throughout the energy band of interest. Since the Mo/Au bilayer films we use have a thickness of $\sim$300 nm, their efficiency at absorbing x-rays diminishes rapidly above 1 keV. In order to maintain the required quantum efficiency over the x-ray band of interest (up to 10 keV) an x-ray opaque absorber must be attached to each TES element. Figure 1

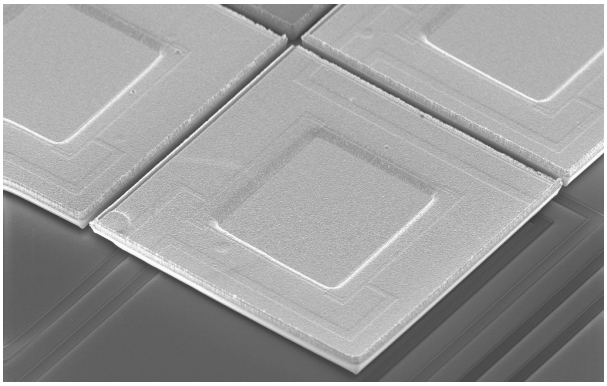

FIGURE 1. Electron micrograph of the mushroom absorbers which, with the TES beneath them, constitute the x-ray microcalorimeter.

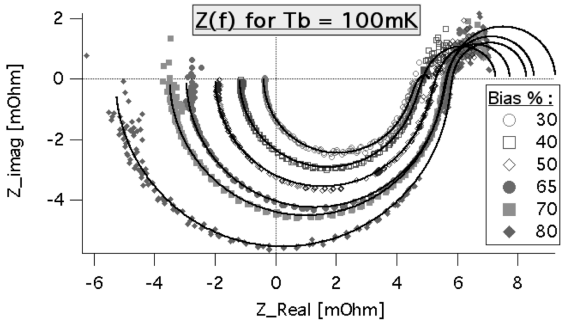

FIGURE 2. Plot of the imaginary versus real components of the microcalorimeter impedance. Each curve corresponds to data taken at a single point in the transition. The dots are data taken at a base temperature of 100 mK, and the black lines are the result of a model fit.

shows an image of the absorbers. We refer to this style of absorber as mushrooms, since they are deposited in such a way that they make contact with the TES, but extend beyond the lateral dimension of the TES to cover the inter-pixel area that contains the wiring leads.

Ideally, the x-ray absorber should be a high Z material, in order to stop the x-rays, but have small heat capacity such that it does not degrade the energy resolution of the microcalorimeter. In addition, a finite thermal conductance $G_{Abs-TES}$ between the absorber and the TES will result in a noise term further degrading the energy resolution; therefore it is important that $G_{Abs-TES}$ be large. Finally, the absorber must also have a large lateral thermal conductivity. Otherwise events absorbed at different location will result in different pulse shapes, leading to a degradation in resolution that is proportional to energy.

The pulse shape and energy resolution equation derived for the simple TES are no longer perfectly valid for such a generalized system. A methodology with which an analytical solution for the more general case may be obtained is described in [4]. Numerical methods can also be used to obtain the response of the generalized microcalorimeter. We have contructed a model that incorporates the main features of the attached absorber microcalorimeter and have determined that is is possible to meet the Constellation-X energy resolution goal of 4 eV with the mushroom absorber design for the desired 250 μm pixel size.

Characterizing the Microcalorimeters

With a good knowledge of the value of the heat capacity, thermal conductances of the various components of the microcalorimeter, as well as the temperature and current dependence of the TES resistance (α and β) a complete physical model of the microcalorimeter can be constructed. The thermal conductivity between the TES and the heat bath can be measured directly from the variation of the IV characteristics with base temperature. Measuring the complex impedance, as a function of frequency, of the microcalorimeter allows us to extract the remaining parameters by fitting the modeled impedance curves to the data. A derivation of the frequency dependent impedance for the simple TES case is given in [5] and [6], while [4] describes how to obtain the impedance for a more general case. Figure 2 shows a plot of the imaginary versus real components of the impedance. Each curve corresponds to a frequency range of $\sim$10 Hz–10 kHz taken at a specific point in the TES transition.

Taking the impedance data for two different values of the base temperature allows us to verify that our fitted parameter results make sense as shown in Figure 3. Using the parameter values obtained from the impedance fits, we were able to determine that the simulated pulse shapes agreed with the data pulses.

Excess Noise and Resolution Performance

The resolution with which the energy of an x-ray can be measured is determined by the thermal and electrical fluctuations in the various components of the microcalorimeter. The individual noise contributions can be calculated based on the equations governing electrothermal feedback. Various groups working on TES-based microcalorimeters have observed larger than expected noise in the devices. Measurements have shown that an additional white noise term, similar to the Johnson noise of the TES resistance, is sufficient to reproduce the properties of the observed noise spectrum. This component, referred to here as *excess* noise appears to be primarily dependent on the point in the superconducting transition

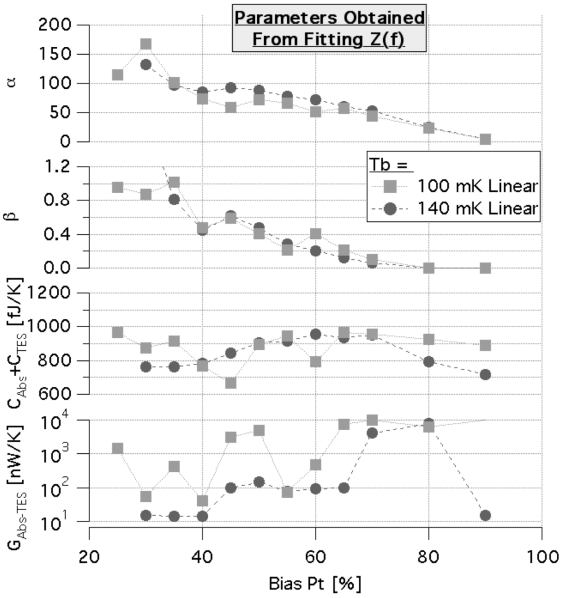

FIGURE 3. Plot of the microcalorimeter parameters which were determined from fitting the impedance data. The squares/circles correspond to fitting the 100/140mK data.

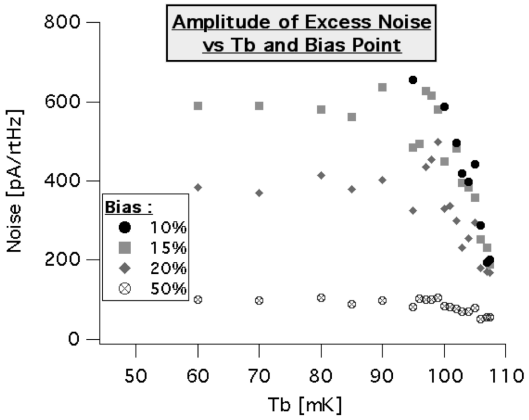

FIGURE 4. Amplitude of the excess noise term, measured in the 2–3 kHz band, as a function of base temperature. The four families of point correspond to the TES being operated at 10, 15, 20, and 50% of the transition. For base temperature more than 10 mK lower than T_c, it can be seen that the noise ceases to vary.

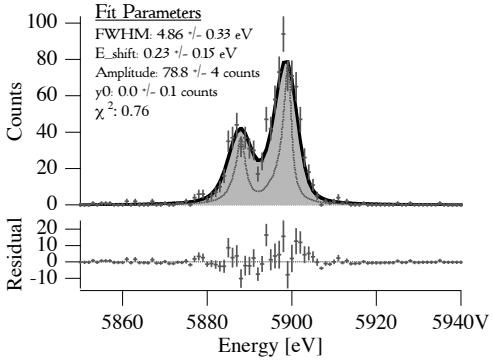

FIGURE 5. Energy spectrum of a Mn Kα fluorescence line obtained by a single pixel TES meeting the size specifications of the Constellation-X mission. The energy resolution at 5.9 keV is determined to be 4.9 eV.

at which the TES is operated, generally increasing significantly as the operating point is lowered in the transition.

By operating the TESs at a base temperature close to T_c, we have observed a decrease in the amplitude of the excess noise term, for a TES operated at the same point in its transition. Figure 4 shows the behavior of the excess noise component at four points in the transition. Within ~ 10 mK of T_c, the amplitude decreases rapidly, while for lower base temperatures it appears to be constant.

Unfortunately, TESs cannot be operated as microcalorimeters so close to their T_c. It has been observed empirically that normal metal bars patterned across the surface of the TES serve to reduce the amplitude of the excess noise component [7]. The sharpness of the transition, α, is also decreased; however, the net effect is improved resolution. By applying the scheme to our TESs, we were able to obtain an energy resolution of 4.9 eV at the 5.9 keV energy of the Mn Kα fluorescence line as shown in Figure 5.

POSITION SENSITIVE TRANSITION EDGE SENSORS

As larger array sizes (beyond kilopixels) become necessary to achieve the field of view and angular resolution requirements of the X-ray telescopes, the approach of using a TES as a single pixel microcalorimeter runs into some challenges. Primary among them are the area on chip required to bring out the wiring from the central pixels, the increased heat dissipation on chip due to the large number of biased TESs, and the increased number of channels required to readout the TESs.

The Position Sensitive TESs (PoST) concept addresses these issues by providing both a position and an energy measurement of the absorbed x-ray. This is done by attaching a TES to either end of a chain of absorbers, ~ 10 pixels long, and comparing the signals seen in the two TESs in order to determine the position of the absorbed x-ray [8]. Figure 6 shows a schematic of the PoST; the vertical stack of absorber, TES, and the thermal impedances in between is equivalent to a single pixel microcalorimeter. The chain of absorber pixels are connected to each other by weak thermal links

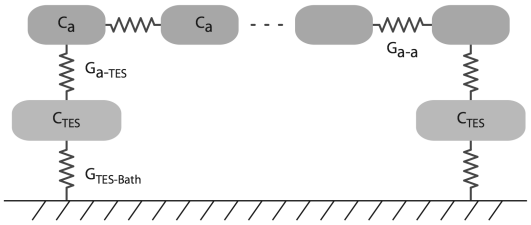

FIGURE 6. Schematic of a PoST thermal model. The rounded boxes represent the x-ray absorbers each of which has a heat capacity C_a and is connected to a neighboring pixel by a thermal conductance G_{aa}. The wider boxes represent the TESs at either end of the PoST and are connect to the edge absorber and the heat bath by G_{a-TES} and $G_{TES-Bath}$.

(G_{aa}). Controlling the value of G_{aa} is necessary to ensure that each absorber pixel is allowed to thermalize before a significant amount of heat travels to the TESs on either side. This ensures that pulses from events absorbed at any point in a given absorber look the same, effectively limiting the position resolution to the size of the absorber while ensuring that the energy resolution is not degraded due to pulse shape variation.

Figure 7 shows data taken with a seven pixel absorber using a KCl fluorescence x-ray source. By plotting the areas of the pulses in TES B against the ares of the pulses in TES A, seven distinct spectra can be seen. The direction parallel to the $y = x$ line corresponds to the sum of the two pulse areas and is proportional to the event energy.

An energy resolution of 11.5 eV at 3.3 keV was obtained from the central pixel, while the resolution of the pixels to either side degraded slowly, but remained within 10% of the central value. The resolutions for each pixel are listed in table 2.

TABLE 2. Energy resolution of the 7 absorbers in a single PoST. The second column lists the measured energy resolution of the K Kα line (3.3 keV) while the third column list the resolution of the Mn Kα line (5.9 keV). A baseline resolution of 8.1 eV was determined from the average pulse shape and noise spectrum.

Pixel Num [μm]	**K Kα Resolution** [eV]	**Mn Kα Resolution** [eV]
1	8.9	10.5±1.3
2	9.1	10.7±1.1
3	9.1	12.3±1.1
4	8.5	8.8±0.64
5	8.9	9.1±0.53
6	9.3	13.2±0.64
7	8.1	13.4±1.2

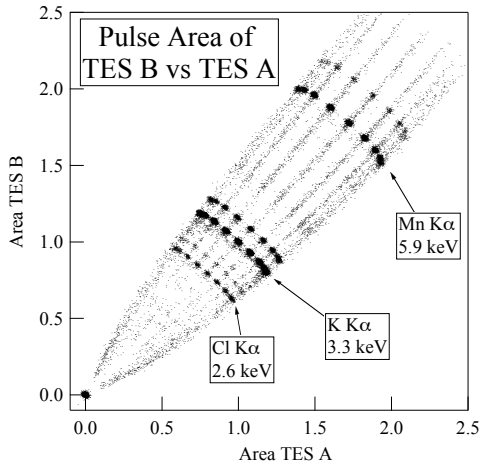

FIGURE 7. Area of the pulse from TES A *vs* TES B, in arbitrary units. Each diagonal line corresponds to a spectrum from a given absorber. The largest peaks in the spectra are due to 2.6, 3.6, and 5.9 keV x-ray lines, while the continuum goes up to 8 keV.

REFERENCES

1. F. B. S. Paerels and S. M. Kahn, *ARA&A*, **41**, 291–342 (2003).
2. H. Inoue, "Astro-E2 mission: the third X-ray observatory in the 21st century," in *X-Ray and Gamma-Ray Telescopes and Instruments for Astronomy*, edited by J. E. Truemper, and H. D. Tananbaum, Bellingham : SPIE, WA, 2003, pp. 289-292.
3. K. D. Irwin, *Phonon-Mediated Particle Detection Using Superconducting Tungsten Transition-Edge Sensors*, Ph.D. thesis, Stanford University, Stanford, CA 94305 (1995).
4. M. Galeazzi and D. McCammon, *Journal of Applied Physics*, **93**, 4856–4869 (2003).
5. M. A. Lindeman, S. Bandler, R. P. Brekosky, J. A. Chervenak, E. Figueroa-Feliciano, F. M. Finkbeiner, M. J. Li, and C. A. Kilbourne, *Review of Scientific Instruments*, **75**, 1283–1289 (2004).
6. J. E. Vaillancourt, *Review of Scientific Instruments*, **76**, 043107 (2005).
7. J. N. Ullom, W. B. Doriese, G. C. Hilton, J. A. Beall, S. Deiker, W. D. Duncan, L. Ferreira, K. D. Irwin, C. D. Reintsema, and L. R. Vale, *Applied Physics Letters*, **84**, 4206–4208 (2004).
8. C. Hammock, E. Figueroa-Feliciano, E. Apodaca, S. Bandler, K. Boyce, J. Chervenak, F. Finkbeiner, R. Kelley, M. Lindeman, S. Porter, T. Saab, and C. Stahle, *Nuclear Instruments and Methods in Physics Research A*, **520**, 505–507 (2004).